J. Korean Inst. Electr. Electron. Mater. Eng.
Vol. 36, No. 4, pp. 418-421 July 2023
DOI: https://doi.org/10.4313/JKEM.2023.36.4.15
ISSN 1226-7945(Print), 2288-3258(Online)

Early Stage Report : Graduate Research

Analysis of Conductivity Variation and Conduction Mechanism in Bulk NiO Based on Sintering Conditions

Ju-Hyeon Lee, Tae-Soo Yeo, and Wook Jo

Department of Materials Science and Engineering, Ulsan National Institute of Science and Technology (UNIST), Ulsan 44919, Korea

(Received May 31, 2023; Revised June 8, 2023; Accepted June 9, 2023)

Abstract: Multilayer Ceramic Capacitors (MLCCs) are essential passive components in the electronics industry, known for their high capacitance due to the multilayer structure comprising inner electrodes and dielectric layers. Nickel electrodes are commonly used in MLCCs as the inner electrodes, and to prevent oxidation during the co-firing of the dielectric layers with nickel electrodes, reducing atmosphere is required. However, reducing atmosphere sintering can also induce a reduction of the dielectric, necessitating precise control of oxygen partial pressure. To explore the possibility of using oxide electrodes that do not require reducing atmosphere sintering, we analyze the electrical properties of nickel oxide (NiO) as a potential candidate. As a preliminary study on its use as an alternative inner electrode, the correlation between microstructure and electrical properties of bulk NiO under different sintering conditions was investigated to gain insights into the conduction mechanisms of the material.

Keywords: MLCC, Inner electrode, Nickel oxides, Conductivity

With the rapid advancement of the electronics industry, passive components such as Multilayer Ceramic Capacitors (MLCCs) have gained equal importance alongside active components like semiconductors. MLCCs play a crucial role in stabilizing the current flowing into active components by providing immediate charge and discharge capabilities, making them essential components in electronic devices [1,2]. A single smartphone can contain approximately 2,000 pcs of MLCCs, highlighting their indispensability in electronic devices. MLCCs differ from disk ceramic capacitors in their multilayer structure, which allows for the parallel connection of multiple dielectric layers, enabling high capacitance within a single component. To facilitate this parallel structure, MLCCs require inner electrodes, as shown in Fig. 1. While silver (Ag) and palladium (Pd) were commonly used as inner electrodes in the past, nickel (Ni) is now widely employed due to considerations of cost and mass production feasibility [3]. Using Ni is a highly efficient way to reduce manufacturing costs because the cost of internal electrodes has increased in proportion to the overall cost due to the decrease in the size of MLCC.

MLCCs are fabricated by various procedures such as making a ceramic slurry, tape casting, screen printing the inner electrode, stacking and lamination, dicing, sintering the green body, and external electrodes dipping and firing [1]. To utilize nickel as the inner electrode, the atmosphere during sintering should be strictly controlled because nickel can be easily oxidized in the air. In order to prevent oxidation of the nickel electrode, sintering should be carried out in a reducing atmosphere [3,4]. However, reducing atmosphere sintering may also induce a reduction of the ceramic dielectric, leading

✉ **Wook Jo; wookjo@unist.ac.kr**

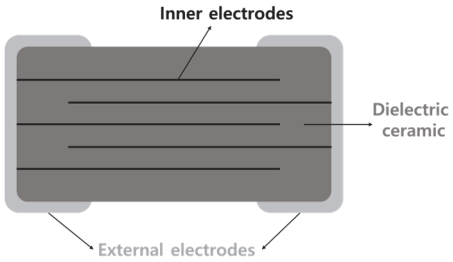

Fig. 1. Schematic of the MLCC structure in the view of a cross-section.

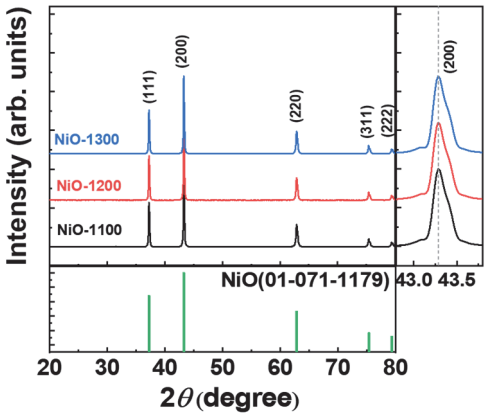

Fig. 2. X-ray diffraction data of NiO according to different sintering temperatures.

to the formation of oxygen vacancies within the dielectric ceramic material. These oxygen vacancies can negatively impact the performance and reliability of the MLCC [5,6]. Thus, it is crucial to prevent the formation of oxygen vacancies by either a reoxidation process or by precisely controlling the oxygen partial pressure. In this wise, there is the predicament of preventing both the reduction of the dielectric and the oxidation of the nickel electrodes during the co-firing of them.

Considering these challenges, some propose that even if nickel oxidizes and forms nickel oxide (NiO), it could still function as an electrode, thereby potentially resolving this issue. To develop NiO as an oxide electrode with enhanced conductivity, it is crucial to analyze the conductivity variations and identify the factors that contribute to increased conductivity in NiO. Therefore, we performed an analysis of the conductivity changes and conduction mechanisms in bulk NiO under different sintering conditions as a preliminary investigation. In this paper, we analyze the correlation between microstructure and electrical properties to provide insights into the conduction mechanisms of the material.

The disk shape of bulk NiO was formed using NiO raw powder (99%, Alpha Aesar). The powder was mixed with 5 wt% of polyvinyl alcohol (PVA) binder to maintain the bonding between particles forming a disk shape. The resulting powder was sieved to under 150 μm particle size and pressed into 10 mm of green ceramic pellets using a die press. The green ceramic pellets were sintered from 1,100℃ to 1,300℃ (NiO-T: T = 1,100, 1,200, 1,300; sintering temperature) for 2 hours in the air after having a binder burnout process at 650℃ for 2 hours.

The purity and crystal structure analysis of the bulk NiO sintered at different temperatures were examined by using X-ray diffraction (XRD) using an X-ray diffractometer (D8 ADVANCE, Bruker AXS, Billerica, Massachusetts, USA) with Cu-Kα radiation as shown in Fig. 2. The absence of impurity peaks in all samples indicates the high purity of the nickel oxide. The NiO has rock-salt symmetry (space group $Fm\bar{3}m$) given that it has (111), (200), (220), (311), and (222) crystal planes, which is in accordance with that of reference spectrum (JCPDS No.01-071-1179). Given that there is no visible shift in the position of the magnified (200) peak for each sample at different sintering temperatures, it can be concluded that there are no significant changes in lattice parameter expansion as the sintering temperature increases. According to Bragg's law ($n\lambda = 2d\sin\theta$) and $d = a/(h^2 + k^2 + l^2)^{1/2}$, the lattice parameter of NiO at each sintering temperature is the same at 4.177 Å.

The microstructure analysis was carried out using scanning electron microscopy (SEM, Quanta 200 FEG, FEI Company, Hillsboro, USA) provided with a backscattered electron (BSE) detector. The BSE (backscattered electron) images of the fracture surfaces of bulk NiO reveal a tendency to increase grain size with increasing sintering temperature (Fig. 3). Under the same sintering time of 2 hours, samples sintered at 1,100℃ exhibited an average grain size of 0.9 μm, while those sintered at 1,200℃ and 1,300℃ showed average grain sizes of 1.6 μm and 2.6 μm, respectively, demonstrating a linear increase in grain size with sintering temperature. Although grain size varied with sintering temperature, the density remained nearly constant at 6.72~6.75 g/cm^3, indicating that densification does not always accompany grain growth [7]. The calculated theoretical density of NiO based on the lattice parameters obtained from XRD is 6.80 g/cm^3, and the relative densities of NiO-1,100, 1,200, and 1,300 are 99.2%, 98.7%,

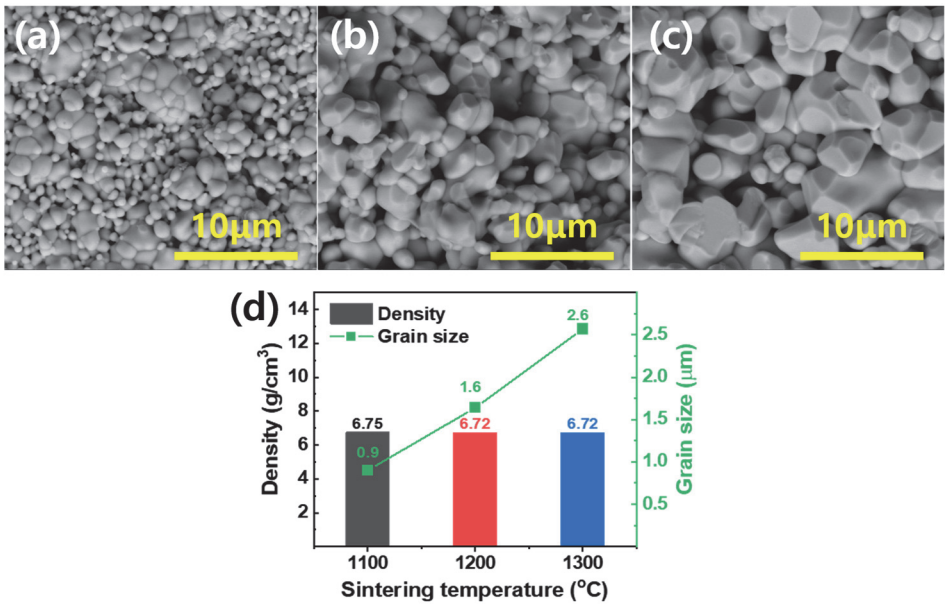

Fig. 3. Backscattered secondary electron (BSE) images of fractured surfaces of (a) NiO-1,100, (b) NiO-1,200, (c) NiO-1,300, and (d) density and grain size of NiO according to the sintering temperatures.

and 98.7%, respectively. This result indicates that sufficient densification has occurred at every sintering temperature, confirming the successful compaction of the NiO.

By analyzing the crystal structure and microstructure, it was observed that the sintering temperature has an influence on the grain size of NiO. To investigate the changes in electrical properties corresponding to these microstructural variations, DC conductivity measurements were performed using a resistance meter (RM-3541, HIOKI, Japan) at room temperature. According to Fig. 4, the conductivity of NiO decreases with increasing sintering temperature, indicating that samples with smaller grain sizes exhibit higher conductivity compared to those with larger grain sizes.

In general, in polycrystalline oxides, grain boundaries have higher resistance than grains, leading to insulating behavior and acting as barriers to conductivity [8-10]. Consequently, when the grain size decreases and the proportion of grain boundaries increases, the local resistance increases, resulting in decreased conductivity [11]. However, in contrast to this general trend, the association between grain size and conductivity in NiO observed in this study shows that grain boundaries do not act as hindrances to conductivity but rather enhance it. This unconventional behavior suggests the need to focus on the conductivity mechanism of NiO. NiO is a p-type semiconductor, which means positive holes serve as the charge

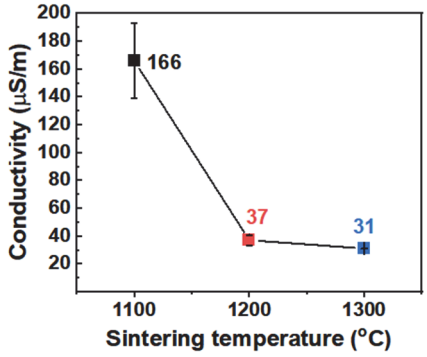

Fig. 4. DC conductivity of NiO-1,100, 1,200, and 1,300.

carriers [12,13]. This occurs due to the formation of positive charges, such as holes ($h^{\bullet}$) or localized holes either on oxygen ($O_O^{\bullet}$, O^-) or on nickel atoms ($Ni_{Ni}^{\bullet}$, Ni^{3+}), for charge compensating the negatively charged intrinsic acceptors (V_{Ni}'' and O_i'') caused by the imperfect stoichiometry of NiO [14,15]. The charge neutrality condition in NiO can be written as

$$[V_{Ni}''] + [O_i''] \rightarrow 2[h^{\bullet}] + [Ni_{Ni}^{\bullet}] + [O_O^{\bullet}] \quad (1)$$

These holes accumulate at grain boundaries, which can then become conductive channels. This observation is supported by previous studies utilizing scanning transmission electron

microscopy coupled with electron energy loss spectroscopy (STEM-EELS), which confirmed the enrichment of oxygen holes ($O_O^{\bullet}$) at NiO grain boundaries [16]. Through these findings, the correlation between microstructure and electrical properties was analyzed, providing insights into the factors influencing conductivity and the underlying conductivity mechanism of the material. In future research, additional analysis such as X-ray photoelectron spectroscopy (XPS) will be conducted to quantitatively measure the ratio of Ni^{3+} to Ni^{2+} in NiO and determine the concentration of conductivity carriers.

In conclusion, to address the issues that can arise during the simultaneous sintering process of nickel electrodes and dielectric layers in MLCCs, this study analyzed the conductivity variation of NiO based on its sintering conditions as a precursor investigation for replacing the nickel internal electrodes with oxide electrodes. The correlation analysis between microstructural changes and electrical properties with respect to the sintering temperature revealed a different trend in NiO compared to conventional polycrystalline oxides. Contrary to expectations, samples with smaller grain sizes exhibited higher conductivity in NiO, indicating a distinctive role of grain boundaries in conductivity. Specifically, NiO, as a p-type semiconductor, accumulated positively charged particles, such as holes, at the grain boundaries, which then acted as conductive channels. Consequently, samples with smaller grain sizes (with more extensive grain boundary areas) demonstrated higher conductivity. Based on these findings, further investigations will be conducted to enhance the conductivity of NiO by increasing hole carriers under different sintering atmosphere. Further investigation is proceeding to develop highly conductive NiO as an oxide electrode material.

ORCID

Wook Jo https://orcid.org/0000-0002-7726-3154

ACKNOWLEDGMENTS

This research was supported by the Creative Materials Dis covery Program (2020M3D1A2102915) through the National Research Foundation of Korea (NRF) funded by Ministry of Science and ICT.

REFERENCES

[1] K. Hong, T. H. Lee, J. M. Suh, S. H. Yoon, and H. W. Jang, *J. Mater. Chem. C*, **7**, 9782 (2019). [DOI: https://doi.org/10.1039/c9tc02921d]

[2] I. Seo, H. W. Kang, and S. H. Han, *J. Korean Inst. Electr. Electron. Mater. Eng.*, **35**, 103 (2022). [DOI: https://doi.org/10.4313/JKEM.2022.35.2.1]

[3] J. Yamamatsu, N. Kawano, T. Arashi, A. Sato, Y. Nakano, and T. Nomura, *J. Power Sources*, **60**, 199 (1996). [DOI: https://doi.org/10.1016/S0378-7753(96)80011-5]

[4] D.F.K. Hennings, *J. Eur. Ceram. Soc.*, **21**, 1637 (2001). [DOI: https://doi.org/10.1016/S0955-2219(01)00082-6]

[5] K. Albertsen, D. Hennings, and O. Steigelmann, *J. Electroceram.*, **2**, 193 (1998). [DOI: https://doi.org/10.1023/A:1009926916939]

[6] G. Y. Yang, G. D. Lian, E. C. Dickey, C. A. Randall, D. E. Barber, P. Pinceloup, M. A. Henderson, R. A. Hill, J. J. Beeson, and D. J. Skamser, *J. Appl. Phys.*, **96**, 7500 (2004). [DOI: https://doi.org/10.1063/1.1809268]

[7] Y. Iida, *J. Am. Ceram. Soc.*, **41**, 397 (1958). [DOI: https://doi.org/10.1111/j.1151-2916.1958.tb13511.x]

[8] A. Cho, C. S. Han, M. Kang, W. Choi, J. Lee, J. Jeon, S. Yu, Y. S. Jung, and Y. S. Cho, *ACS Appl. Mater. Interfaces*, **10**, 16203 (2018). [DOI: https://doi.org/10.1021/acsami.8b02630]

[9] G. Y. Yang, E. C. Dickey, C. A. Randall, D. E. Barber, P. Pinceloup, M. A. Henderson, R. A. Hill, J. J. Beeson, and D. J. Skamser, *J. Appl. Phys.*, **96**, 7492 (2004). [DOI: https://doi.org/10.1063/1.1809267]

[10] A. Uthayakumar, A. Pandiyan, S. Mathiyalagan, A. K. Keshri, and S.B.K. Moorthy, *J. Phys. Chem. C*, **124**, 5591 (2020). [DOI: https://doi.org/10.1021/acs.jpcc.0c00166]

[11] J. W. Liu, D. Y. Lu, X. Y. Yu, Q. L. Liu, Q. Tao, H. Change, and P. W. Zhu, *Acta Metall. Sin. (Engl. Lett.)*, **30**, 97 (2016). [DOI: https://doi.org/10.1007/s40195-016-0522-y]

[12] H. J. Van Daal and A. J. Bosman, *Phys. Rev.*, **158**, 726 (1967). [DOI: https://doi.org/10.1103/PhysRev.158.736]

[13] M. D. Irwin, D. B. Buchholz, A. W. Hains, R.P.H. Chang, and T. J. Marks, Proc. *Natl. Acad. Sci.*, **105**, 2783 (2008). [DOI: https://doi.org/10.1073/pnas.0711990105]

[14] D. Y. Cho, S. J. Song, U. K. Kim, K. M. Kim, H. K. Lee, and C. S. Hwang, *J. Mater. Chem. C*, **1**, 4334 (2013). [DOI: https://doi.org/10.1039/c3tc30687a]

[15] F. Jiang, W.C.H. Choy, X. Li, D. Zhang, and J. Cheng, *Adv. Mater.*, **27**, 2930 (2015). [DOI: https://doi.org/10.1002/adma.201405391]

[16] R. Poulain, G. Lumbeeck, J. Hunka, J. Proost, H. Savolainen, H. Idrissi, D. Schryvers, N. Gauquelin, and A. Klein, *ACS Appl. Electron. Mater.*, **4**, 2718 (2022). [DOI: https://doi.org/10.1021/acsaelm.2c00230